Organic Geochemistry 52 (2012) 1–12

Contents lists available at SciVerse ScienceDirect

Organic Geochemistry

journal homepage: www.elsevier.com/locate/orggeochem

Kinetics of oil group-type generation and expulsion: An integrated application to Dongying Depression, Bohai Bay Basin, China

Zhifu Wei [a,b], Yan-Rong Zou [a,*], Yulan Cai [a], Lei Wang [a,b], Xiaorong Luo [c], Ping'an Peng [a]

[a] State Key Laboratory of Organic Geochemistry, Guangzhou Institute of Geochemistry, Chinese Academy of Sciences, Guangzhou, GD 510640, China
[b] Graduate University of Chinese Academy of Sciences, Beijing 10039, China
[c] Key Laboratory of Petroleum Resource Research, Institute of Geology and Geophysics, Chinese Academy of Sciences, Beijing 10029, China

ARTICLE INFO

Article history:
Received 6 April 2012
Received in revised form 2 August 2012
Accepted 6 August 2012
Available online 15 August 2012

ABSTRACT

Pyrolysis of two kerogens isolated from the $E_{2\text{-}3}s_3^3$ and $E_{2\text{-}3}s_4^1$ source rocks in the Niuzhuang sag, Dongying Depression, Bohai Bay Basin, China, was performed in a confined system. The products were extracted with solvent and separated using micro-column chromatography into group-type fractions (saturates, aromatics, resins and asphaltenes) with the kerogen residue in each case undergoing swelling with a variety of solvents. The kinetics for generation and retention of crude oil and its group-type fractions from the kerogens were studied and the kinetic parameters applied to modeling generation and retention of crude oil and its fractions from the $E_{2\text{-}3}s_3^3$ and $E_{2\text{-}3}s_4^1$ source rocks on the basis of burial and thermal history of the Niuzhuang sag. The results show that the "normal oil" was generated at about 4.26 Ma and 24.85 Ma ago, but expelled at about 3.96 Ma and 17.46 Ma ago, respectively, from $E_{2\text{-}3}s_3^3$ and $E_{2\text{-}3}s_4^1$ source rocks. The current proportions of the expelled saturates, aromatics and NSOs are about 60%, 15% and 25%, respectively.

1. Introduction

Petroleum formation from source rocks is generally attributed to progressive catagenesis of kerogen and bitumen with increasing temperature and depth of burial in sedimentary basins (Tissot and Espitalié, 1975). Since numerous reactions occur in source rocks, simulation requires products to be grouped and assumptions to be made for modeling cracking kinetics. Several models have been described (Lopatin, 1971; Tissot and Espitalié, 1975; Quigley et al., 1987; Burnham and Braun, 1990; Braun and Burnham, 1990, 1992; Behar et al., 1991a,b, 1997; Pepper and Corvi, 1995a; Pepper and Dodd, 1995). It is widely accepted (Tissot and Welte, 1984) that thermal evolution of petroleum is controlled by the kinetics of cracking reactions that occur in sedimentary basins at low temperature (100–200 °C) over time (typically a few million years). Detailed information about such alteration is of prime importance in relation to exploration of petroleum resources and prediction of oil and gas quantity and quality. Such processes are simulated under laboratory conditions, i.e., at higher temperature, usually between 250 and 600 °C, since under such conditions reactions are sufficiently rapid that cracking can be monitored within an acceptable time frame (Tissot and Espitalié, 1975; Burnham and Braun, 1990; Ungerer, 1990; Behar et al., 1991a,b, 1997; Horsfield et al., 1992; Lewan, 1993; Schenk et al., 1997a,b; Waples, 2000). Empirical kinetic schemes, commonly used by petroleum geochemists, consist of determination of global stoichiometric equations that can be extrapolated to basin temperatures, assuming that cracking reactions follow a first order kinetic law, in which the rate of kerogen degradation, dc/dt, is proportional to the concentration c_0 of oil,

$$dc_0/d_t = -k_0 c_0 \quad (1)$$

The rate constant k is described by the Arrhenius equation:

$$k_0 = A_0 \exp(-E_0/RT) \quad (2)$$

where A is the frequency factor (s^{-1}), E the activation energy ($J\ mol^{-1}$), R (8.31441 $J\ mol^{-1}\ K^{-1}$) the universal gas constant and T the absolute temperature (K). For a given reaction, A may be conceptually considered to be proportional to the vibrational frequency of the reactants, whereas E is proportional to the bond energy.

Kinetic laws are therefore routinely considered as the mathematical links between high temperature, short-time and low temperature, long-time configurations, allowing extrapolation from laboratory to natural heating conditions.

Pyrolysis techniques are frequently used to study oil and gas generation under controlled laboratory conditions. With the introduction of mathematical kinetic models, hydrocarbon formation in experiments can be accurately modeled and the resulting kinetic parameters can be extrapolated to predict the rate and timing of hydrocarbon generation in sedimentary basins (Braun and Burnham, 1990; Burnham and Braun, 1999).

It has been shown that coals are macromolecular systems which can be studied by techniques developed in polymer science

* Corresponding author. Tel.: +86 20 85290187; fax: +86 20 85290706.
E-mail address: zouyr@gig.ac.cn (Y.-R. Zou).

0146-6380/$ - see front matter © 2012 Elsevier Ltd. All rights reserved.
http://dx.doi.org/10.1016/j.orggeochem.2012.08.006

(Takanohashi et al., 1996, 2000; Cody and Painter, 1997; Otake and Suuberg, 1997) and their application to primary migration (Sandvik et al., 1992) and kerogen (Larsen and Li, 1997a,b) has been attempted. One object of this study was to apply the swelling theory to predict retention and expulsion of petroleum and its fractions. In past years, many kinetic studies of oil and gas generation have been carried out, but few focused on the kinetics of petroleum and its fractions. Here, both total products and their fractions were analyzed to obtain kinetic parameters, which were then extrapolated to geological conditions. Generation, retention and expulsion of the total products and their group-based fractions are also discussed.

2. Geological background

The Dongying Depression lies in the southeast of the Bohai Bay Basin and has an area of 5850 km^2 (Fig. 1A). It is one of the most oil rich rift areas in the east of China. In total, 32 oilfields and 2 gas fields have been discovered, with the total petroleum reserve being estimated at 23.4E+8 tons.

The depression is an asymmetric "dustpan-shaped" lacustrine basin (Fig. 1B). It can be divided into five secondary tectogenes from north to south, i.e., steep slope zone, northern sag zone, central anticline zone, south sag zone and gentle slope zone (Wang and Qian, 1992). According to the tectonic history and sedimentary sequences, the basin evolution can be divided into three stages: (i) pre-rift stage, when Lower Paleozoic marine platform sediments and Upper Paleozoic paralic facies of coal measures were developed on the Precambrian crystalline basement, (ii) rift stage, when abundant Mesozoic and Paleogene fluvial–lacustrine sediments were deposited, and (iii) depression stage, when Neogene fluvial sediments were developed (Pan et al., 2003). Geochemical evidence supports the conclusion that the Paleogene lacustrine sediments at the rift stage are the main hydrocarbon source rocks (Wang and Qian, 1992; Chen et al., 1994; Zhang et al., 2003).

The Paleogene stratigraphy in the depression comprises the Kongdian ($E_{1\text{-}2k}$), Shahejie ($E_{2\text{-}3s}$) and Dongying (E_{3d}) formations (Fig. 1B). Detailed descriptions of the Paleogene stratigraphy have been presented by authors such as Pang et al. (2003) and Zhang et al. (2004). Studies suggest that three sub-members of $E_{2\text{-}3}s$, including the upper $E_{2\text{-}3}s_4$, lower $E_{2\text{-}3}s_3$ and middle $E_{2\text{-}3}s_3$, are the main source rocks. The upper $E_{2\text{-}3}s_4$ member consists of brackish to saline lacustrine sediments with a thickness of about 40–300 m. The lithology is dominated by brownish-gray, gray to black shales, calcareous mudstones and mudstones, intercalated with light gray to gray dolostone and marlstone. The lower $E_{2\text{-}3}s_3$ member consists of brackish to fresh water lacustrine sediments with a thickness of about 100–300 m. The main lithology corresponds to gray to black shales, gray to black calcareous mudstones and mudstones. The middle $E_{2\text{-}3}s_3$ member consists of freshwater lacustrine to prodelta sediments with a thickness of 300–500 m. The main lithology corresponds to gray to black calcareous mudstones and mudstones (Wang et al., 1992; Liu et al., 2003).

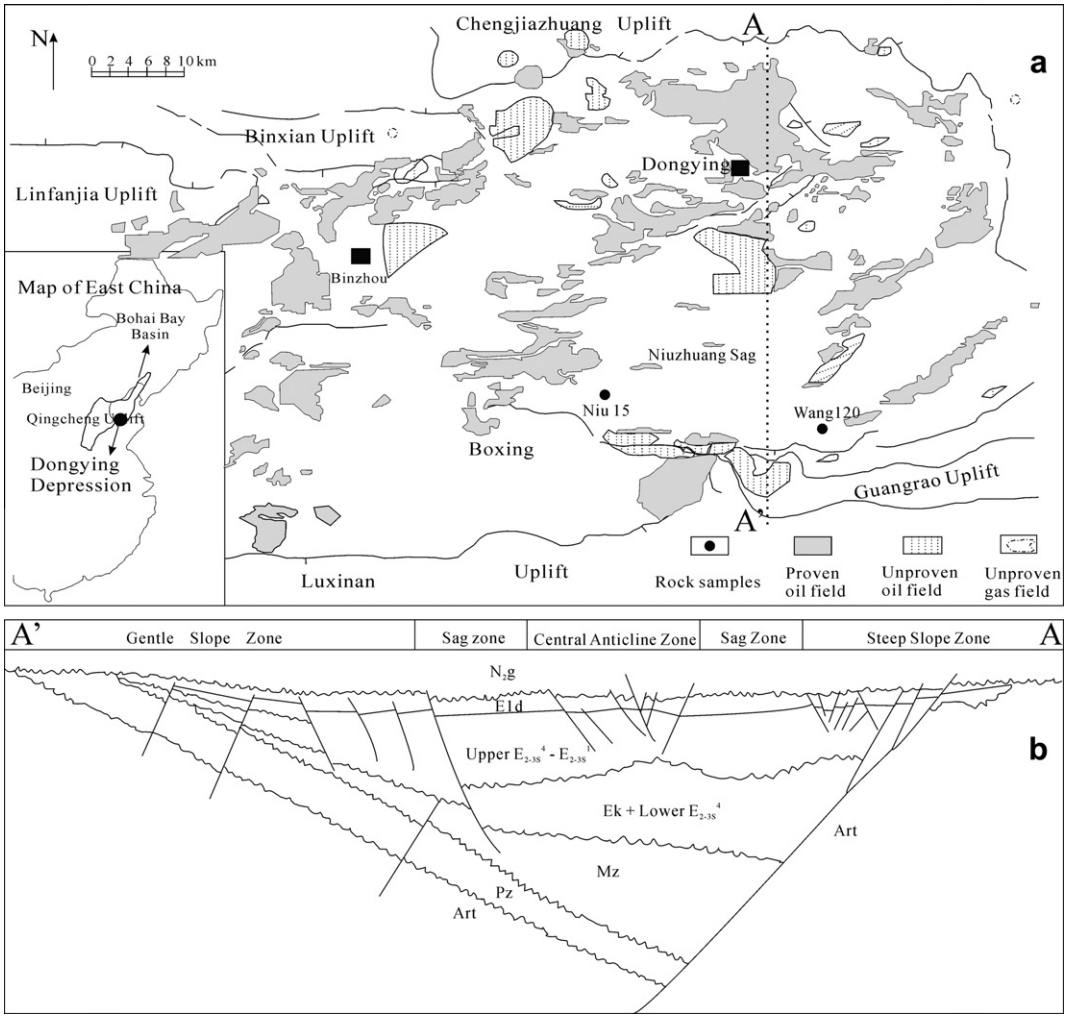

Fig. 1. Oil and gas fields (a) and N–S structural cross-section (b) in the Dongying Depression, Bohai Bay Basin, China (after Li, 2004; Zhang et al., 2009).

The source rocks are mainly confined to three stratigraphic intervals, i.e., lower Sha-3($E_{2\text{-}3}s_3^3$), middle Sha-3($E_{2\text{-}3}s_3^2$) and upper Sha-4 Members ($E_{2\text{-}3}s_4^1$), which can be divided into two types. One is massive mudstone, developed within the high stand system tracts of third-order sequence, the other is oil shale, developed within the transgressive system tracts of the lake. The former is thick (up to several hundred meters) but varies in thickness regionally. In contrast, the latter is thin (generally less <100 m) and has a regular thickness distribution on a regional scale, to such degree that it can be traced over the entire depression. As one of the condensed sections, the oil shale is an excellent source rock since it shows high oil generating potential.

3. Samples and experiments

3.1. Samples

The source rock samples were collected from Well Wang120 and Well Niu15 in the Dongying Depression. The samples were ground to 0.175–0.150 mm (80–100 mesh) and demineralized using HF and HCl, followed by cleaning with distilled water to isolate the kerogen. The total organic carbon (TOC) content of the two kerogens was 85.1% (Niu15) and 49.3% (Wang120). An aliquot (70–100 mg) of each source rock sample was weighed for Rock–Eval VI analysis. The geochemical data for the source rocks are presented in Table 1.

3.2. Pyrolysis

The pyrolysis experiment was conducted in a confined system, following the procedures described in detail by Behar et al. (1991a,b). The kerogen sample (70–100 mg) was sealed in a gold tube (50 mm × 4 mm i.d.), which was welded on one end. The tube was flushed (ca. 15 min) with Ar to insure complete removal of air and the remaining end sealed in an argon atmosphere, using arc welding. Thereafter, the sealed gold cells were put into autoclaves and water (ca. 10 ml) was put into each autoclave that was connected to a pressure waterline. The pressure device consists of an air compressor, and an increment pump which drives high pressure water to fill the autoclaves. The samples in the autoclaves were heated in a single oven to the targeted temperature. During pyrolysis the pressure in the autoclaves was adjusted by adding water from the pump or removing water through a leakage valve.

The pressure was kept at 50 MPa, with an error of <5 MPa being observed during the whole pyrolysis procedure. The temperature was programmed to increase at 2 °C/h and 20 °C/h, respectively, with final target temperatures ranging from 320–420 °C. The heat circulating fan placed at the bottom of the oven can make a difference of <1 °C among the autoclaves. Finally, the autoclaves were removed from the oven one at a time, and quenched in a cold water bath.

The ends of the gold tubes were cut off at ambient temperature (<28 °C), and the samples were removed, wrapped with filter paper and extracted (36 h) in a Soxhlet apparatus with a ternary solvent (MeOH:benzene:acetone, 2:1:1 v:v:v). Finally, the solvent was evaporated from the extracts and the extracts weighed.

3.3. Separation of C_{14+} fractions

Micro-column chromatography is one of the easiest, fastest, most economical and effective methods for separation of crude oil fractions (Bastow et al., 2007). In this study, soluble organic matter extracted from the pyrolyzed kerogen was weighed and separated by using micro-column chromatography into saturates, aromatics, resins and asphaltenes following the procedures described by Xu and Sun (2006). The proportions (%) were calculated by way of normalization; and the yields are listed in Table 2.

3.4. Solvent swelling experiments

Each extracted kerogen sample was introduced into a glass tube (5 × 15 mm), plugged with quartz wool at both ends. The tube was immersed into organic solvent (30 °C, 24 h) and centrifuged at 4000 rpm for 10 min. The initial weight (w_1) and swollen weight (w_2) could be determined by electronic microbalance, the subtraction method applied and the swelling behavior of the solvent estimated from the volumetric swelling ratio, which was calculated from the following equation (Hamurcu and Baysal, 1993):

$$Q_v = 1 + \rho_2 * (w_2 - w_1)/\rho_1 * w_1 \quad (3)$$

where w_1 is the initial weight of the kerogen before swelling, w_2 equilibrium weight of the swollen kerogen, ρ_1 and ρ_2 are the density of the solvent and the residual kerogens, respectively. For type I kerogen, the density range is from 1.05–1.25 within the "oil window" according to the density and elemental composition of alginite isolated by density gradient centrifugation (DGC) separation (Han and Krugr, 1999). In this study, the density of the residual kerogens are estimated as 1.15 g/cm^3 by a middle density. The swelling data of the residual kerogens shown in Appendix 1.

4. Results and discussion

4.1. Total hydrocarbon conversion

Petroleum is generated from kerogen with disordered structures, due to heat effect on the various heteroatomic bonds and carbon bonds. Oil and gas generation can occur at a certain temperature range and significant quantities of hydrocarbons would be generated once the temperature threshold is exceeded.

Two heating rates, 20 °C/h and 2 °C/h, were selected for kerogen pyrolysis. Table 2 shows the relationships between pyrolysis temperature and cumulative yields at the two different heating rates and that yield increases progressively with increasing pyrolysis temperature up to the maximum yield. For example, the maximum yield from Niu15 kerogen is reached at 355 °C for 2 °C/h heating rate, while the maximum yield occurs at 380 °C for pyrolysis at a

Table 1
Geochemical data for source rocks from Dongying Depression, Bohai Bay Basin, China.

Sample	Stratum	Age	Lithology	TOC[a] (%)	T_{max}[b] (°C)	S1[c] (mg/g)	S2[d] (mg/g)	S3[e] (mg/g)	HI[f] (mg/g TOC)	OI[g] (mg/g TOC)	Kerogen type
Niu15	Lower Sha-3	$E_{2\text{-}3}s_3^3$	Mudstone	13.12	444	4.34	104.18	0.71	794	5	I
Wang120	Upper Sha-4	$E_{2\text{-}3}s_4^1$	Mudstone	4.72	432	0.99	40.6	0.45	860	10	I

[a] Total organic carbon.
[b] Temperature of maximum release of hydrocarbons from cracking of kerogen.
[c] Amount of free hydrocarbons (gas and oil).
[d] Amount of hydrocarbons generated through thermal cracking.
[e] Amount of CO_2 pyrolysis of kerogen.
[f] Hydrogen index.
[g] Oxygen index.

Table 2
Pyrolysates and group-type composition of Niu15 kerogen and Wang120 kerogen at different temperatures and different heating rates.

Temp. (°C)	Niu15 kerogen ($E_{2\text{-}3}s_3^3$)					Wang120 kerogen ($E_{2\text{-}3}s_4^1$)				
	Pyrolysate (mg/g C)	Saturates (mg/g C)	Aromatics (mg/g C)	Resin (mg/g C)	Asphaltene (mg/g C)	Pyrolysate (mg/g C)	Saturates (mg/g C)	Aromatics (mg/g C)	Resin (mg/g C)	Asphaltene (mg/g C)
Heating rate 2 °C/h										
320	60.83	19.83	10.66	27.55	2.79	140.83	56.72	28.61	45.38	10.12
325	121.13	51.90	22.68	38.71	7.84	210.83	98.45	41.64	52.10	18.63
330	184.18	88.85	34.23	47.12	13.98	298.23	153.74	56.32	58.44	29.73
335	283.55	148.90	53.38	57.21	24.06	377.54	205.03	70.10	62.34	40.07
340	359.11	198.07	66.02	62.90	32.12	438.52	242.60	83.30	65.88	46.75
345	453.21	261.68	81.67	66.67	43.19	492.50	277.28	94.50	68.52	52.20
350	524.52	308.56	95.56	69.79	50.61	511.73	296.27	100.18	60.86	54.42
355	578.66	342.64	107.16	73.38	55.48	447.23	257.88	98.68	49.22	41.45
360	504.00	280.83	114.12	67.18	41.87	385.03	219.39	91.87	45.58	28.20
365	429.44	224.09	118.62	58.00	28.73	340.07	194.25	86.10	40.53	19.19
370	351.16	169.61	119.84	45.39	16.32	302.34	177.29	75.76	36.57	12.71
375	323.85	159.72	110.73	40.90	12.50	273.13	167.76	61.97	31.80	11.60
390	271.95	133.29	94.60	34.95	9.11	234.38	136.12	60.90	26.93	10.43
400	234.42	118.55	80.96	27.63	7.28	221.54	126.59	57.74	26.82	10.39
Heating rate 20 °C/h										
340	46.22	16.77	8.95	18.36	2.13	112.84	46.61	24.01	33.78	8.44
345	73.09	30.18	13.19	25.34	4.37	157.45	72.38	30.32	40.81	13.94
350	108.99	47.61	20.42	33.79	7.18	205.38	100.16	38.86	47.28	19.09
355	162.64	78.11	31.31	41.20	12.03	267.63	139.65	48.15	52.79	27.05
360	225.96	115.73	43.77	48.07	18.39	333.02	180.57	59.69	56.99	35.76
365	317.53	173.26	60.65	55.58	28.05	392.45	219.11	70.02	60.16	43.17
370	388.93	220.25	71.13	61.35	36.19	440.76	248.64	81.38	63.17	47.57
375	460.10	269.66	81.97	64.03	44.44	479.06	279.03	92.96	54.60	52.48
380	524.26	310.71	94.61	67.44	51.49	453.63	264.98	91.66	51.01	45.98
385	494.08	280.98	105.88	63.50	43.72	415.69	246.47	85.12	45.48	38.62
390	444.62	242.48	111.97	55.56	34.61	364.18	212.69	81.59	43.04	26.87
395	403.18	216.17	108.51	50.52	27.98	331.97	194.48	75.90	41.91	19.68
410	304.40	175.49	78.33	35.53	15.05	285.98	163.75	68.05	37.14	17.04
420	211.17	114.84	54.95	32.55	8.83					

faster rate, the maximum yield from Wang120 kerogen is reached at 350 °C and 375 °C for 2 °C/h and 20 °C/h heating rates, respectively. The yield decreases after the maximum is reached, which is associated with secondary hydrocarbon cracking in the confined system. The maximum yield at 2 °C/h is 578.7 mg/g TOC and 511.7 mg/g TOC for Niu15 and Wang120 kerogen, respectively. However, the maximum yield at 20 °C/h is lower than that at 2 °C/h, being 524.3 mg/g TOC and 479.1 mg/g TOC for Niu15 and Wang120 kerogen, respectively.

4.2. Kinetic parameters

Petroleum formation or hydrocarbon generation is a process of progressive transformation, which can be described as a function of time and temperature (Juntgen and Klein, 1975; Tissot and Welte, 1984; Tissot et al., 1987; Schenk et al., 1997a,b), while characterization of hydrocarbon generation of a known organic matter sample can be described by way of chemical kinetics in terms of activation energy and frequency factor. This generation process is accompanied by cracking of numerous covalent bonds (e.g., C–C, C–O, C–S), each having a distinct activation energy. The energy for a given bond type is related to the structure of the source organic matter and the distribution of covalent bonds in its matrix. The progress of hydrocarbon generation can be predicted by determining the activation energy distribution and the frequency factor on the basis of pyrolysis experiments. Conventional kinetic models use either a single activation energy and frequency factor set (Welte and Yalcin, 1988), or multiple activation energies with a single frequency factor (Tissot et al., 1978; Delvaux et al., 1990; Reynolds et al., 1995; Dieckmann, 1998; Schenk and Horsfield, 1998; Vandenbroucke et al., 1999), to model hydrocarbon generation. Models containing a distribution of activation energy values and a distribution of frequency factor values have also been applied (Dieckmann et al., 2002; Dieckmann, 2005).

The yields of the total hydrocarbons and the group-based fractions for the pyrolysates generated from the two kerogens were obtained from the experiment. The experimental data and fitting data of conversion are given in Table 2 and illustrated in Fig. 2, which clearly show that the calculated yields agree well with the measured values. As a result, the kinetic parameters of hydrocarbon generation can be reasonably extrapolated from the laboratory conditions to geological conditions.

Based on the calculated activation energies and frequency factors derived from the kinetic experiments with the kerogens, the experimental data were processed with special kinetics software. The cumulative conversion of the total hydrocarbons or any of the group-based fractions for a certain geological period under a known paleo-geothermal history can be obtained on the basis of information about the thermal history of the source rocks. KINETICS 2000 software was employed to fit the kinetic parameters, including activation energy distributions and frequency factors for the total hydrocarbons, saturates, aromatics, resins and asphaltenes from the two kerogen samples (Fig. 3). It is noted that two heating rates are fitted simultaneously (Fig. 2) and the activation energies (Fig. 3) are derived from a simultaneous fit by KINETICS 2000. Kinetic constants were derived in all cases using a fixed frequency factor for comparison, and manual iterations indicated that a frequency factor of $A = 5.0E{+}15\ s^{-1}$ worked best. As shown in Fig. 3, the Ea of the liquid products generated from the two kerogens exhibit similar distribution patterns varying in the range 55–60 kcal/mol. The difference is that Ea is higher for Niu15 kerogen than for Wang120 kerogen. For example, the predominant Ea is 56 kcal/mol for the total hydrocarbons from Niu15 kerogen (Fig. 3a), but becomes 55 kcal/mol for the total hydrocarbons from

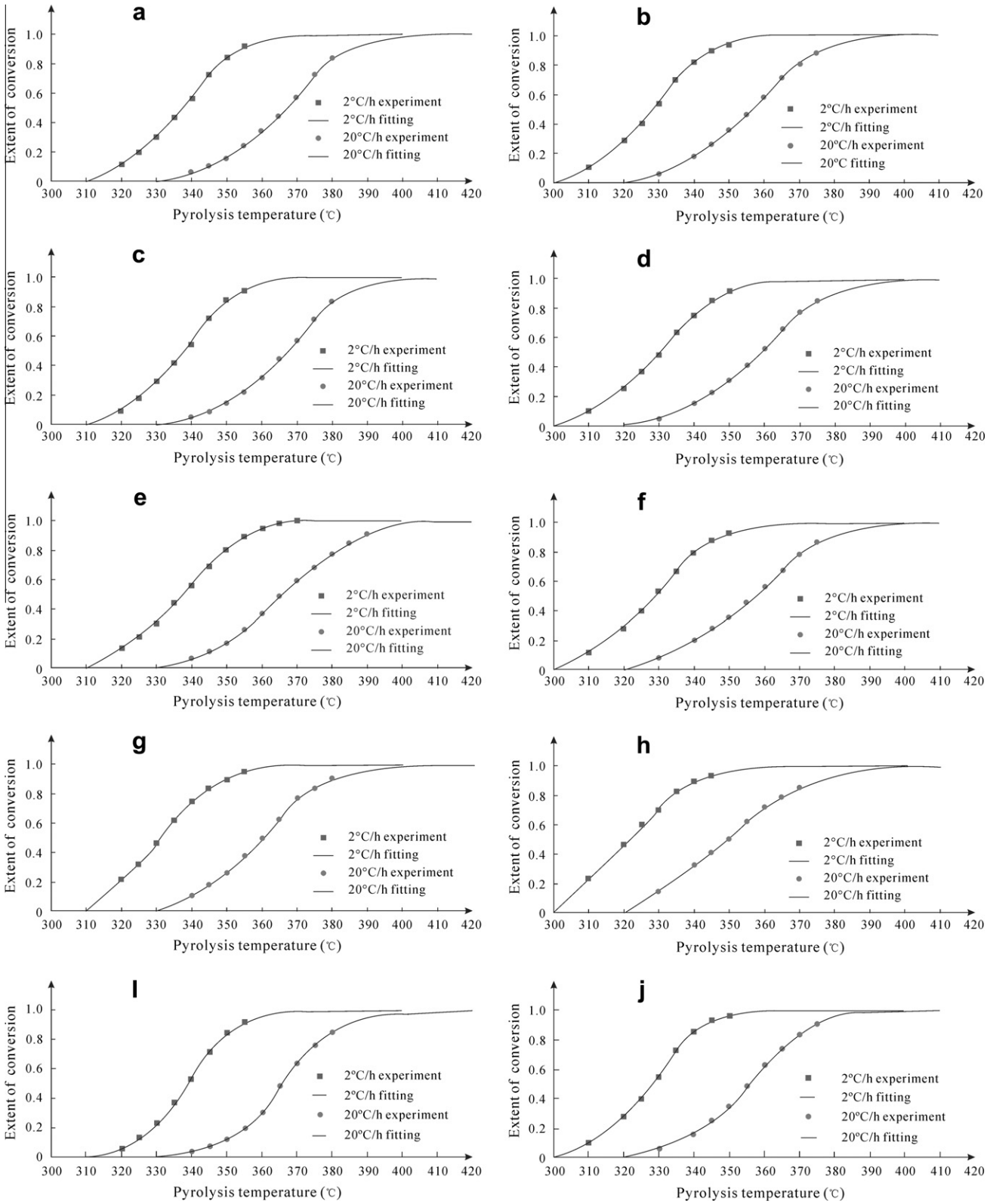

Fig. 2. Experimental and calculated conversion of pyrolysates at heating rates of 2 °C/h and 20 °C/h respectively (a, Niu15 total hydrocarbon; b, Wang120 total hydrocarbon; c, Niu15 saturates; d, Wang120 saturates; e, Niu15 aromatics; f, Wang120 aromatics; g, Niu15 resins; h, Wang120 resins; i, Niu15 asphaltenes; j, Wang120 asphaltenes).

Wang120 kerogen (Fig. 3b). In addition, Ea for the group-based fractions demonstrates a sequence of saturates > aromatics > asphaltenes > resins. Behar et al. (2010) observed that the mean Ea value for Type I kerogen is 56 kcal/mol, corresponding to an A value of 5.64E+14 s^{-1}, as Ea ranges from 48 to 66 kcal/mol, while others (Ungerer and Pelet, 1987; Braun et al., 1992; Sundararaman et al., 1992) found that the mean value of Ea for Type I kerogen is 54 kcal/mol. Therefore, our results are very close to the parameters found by previous researchers for Type I kerogen.

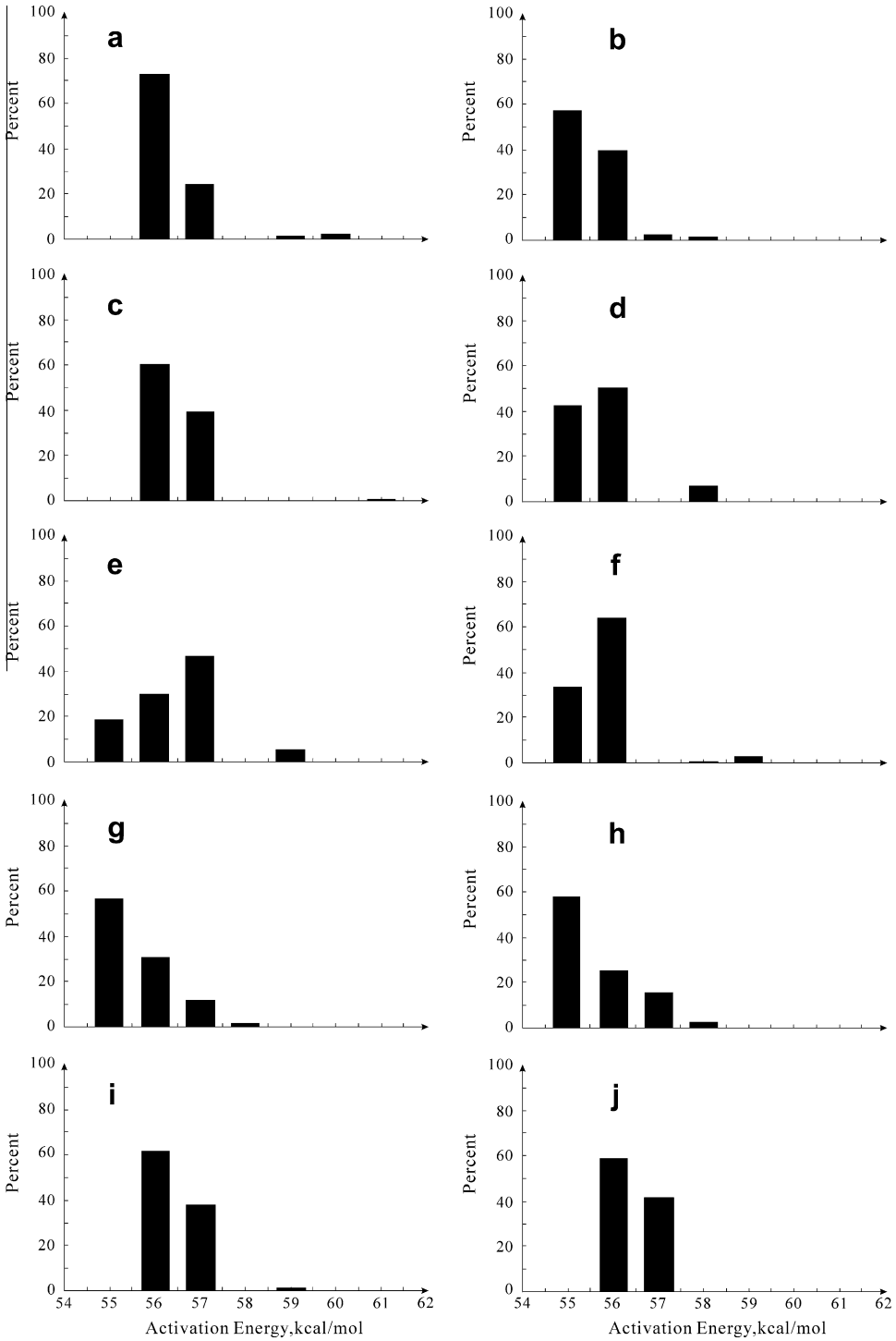

Fig. 3. Kinetic parameters for products generated from kerogen pyrolysis (a, Niu15 total hydrocarbon; b, Wang120 total hydrocarbon; c, Niu15 saturates; d, Wang120 saturates; e, Niu15 aromatics; f, Wang120 aromatics; g, Niu15 Resins; h, Wang120 resins; i, Niu15 asphaltenes; j, Wang120 asphaltenes). Note: 1 kcal/mol = 4.2 kJ/mol). For comparison, the pre-exponential factor is fixed as $A = 5.0000E+15\ s^{-1}$ in all cases.

4.3. A geological application

4.3.1. Hydrocarbon generation history

When organic matter is affected by a variety of factors, such as paleotemperature and geological time, complicated chemical reactions occur and finally result in petroleum generation. These reactions are actually chemical processes occurring on the geological time scale. It is generally assumed that a reaction occurring under geological conditions would show similar chemical kinetic properties (e.g., activation energy E and frequency factor A) to the reaction occurring under controlled conditions in the laboratory. Therefore, based on the kinetic parameters acquired from the laboratory experiments for hydrocarbon generation, geochemical processes of hydrocarbon generation can be simulated and reproduced (Behar et al., 1991a,b; Tang et al., 1996).

The Niuzhuang sag is in the southern part of the depression, which is a secondary level sag in the Dongying Depression (Fig. 1). The Cenozoic stratigraphy in the sag consists mainly of

two sets of source rocks $E_{2\text{-}3}s_3$ and $E_{2\text{-}3}s_4$, and the dark mudstone of lower $E_{2\text{-}3}s_3$ ($E_{2\text{-}3}s_3^3$) and upper $E_{2\text{-}3}s_4$ ($E_{2\text{-}3}s_4^1$) is the major source rock, with a maximum thickness of about 900 m. The $E_{2\text{-}3}s_4^1$ member consists of brownish-gray, gray to black shales with a thickness of about 200 m, and the $E_{2\text{-}3}s_3^3$ member consists of gray to black shales and mudstones with a thickness of about 600 m.

The Cenozoic stratigraphy in the sag experienced continuous subsidence (Fig. 4; Zhang et al., 1999). Studies have shown that the ancient temperature at the land surface of the Dongying Depression was 14 °C and the ancient geothermal gradient 36 °C/km (Editing Committee of Chinese Petroleum Geology, 1987; Zhang et al., 1999). When the parameters derived for Niu15 kerogen are applied to source rocks of $E_{2\text{-}3}s_3^3$ and the parameters for Wang120 kerogen to source rocks of $E_{2\text{-}3}s_4^1$, the hydrocarbon generating history of the Niuzhuang sag, Dongying Depression can be modeled. The results are indicated in Figs. 5 and 6.

The degree to which kerogen is transformed to hydrocarbons is the transformation ratio, which can be measured based on the kinetics of the transformation process. Oil generation can be commonly gauged by the value of the transformation ratio and divided into three stages, i.e., early generation, main phase and late generation, corresponding respectively to a transformation ratio (fraction) of 0.10–0.25, 0.25–0.65 and 0.65–0.90 (Houseknecht and Hayba, 1998). In addition, a transformation ratio of 0.10 can be established for bulk kinetic analysis of kerogen to mark the onset of hydrocarbon formation by using kinetic extrapolations (Pepper and Corvi, 1995a). As shown in Fig. 5, the maximum fraction reacted for $E_{2\text{-}3}s_3^3$ and $E_{2\text{-}3}s_4^1$ source rocks is 0.63 and 0.98, respectively, so the source rocks of $E_{2\text{-}3}s_3^3$ are in the main phase of hydrocarbon generation, while the $E_{2\text{-}3}s_4^1$ source rocks have basically completed oil generation. It can also be predicted that the source rocks of $E_{2\text{-}3}s_3^3$ and $E_{2\text{-}3}s_4^1$ entered their oil

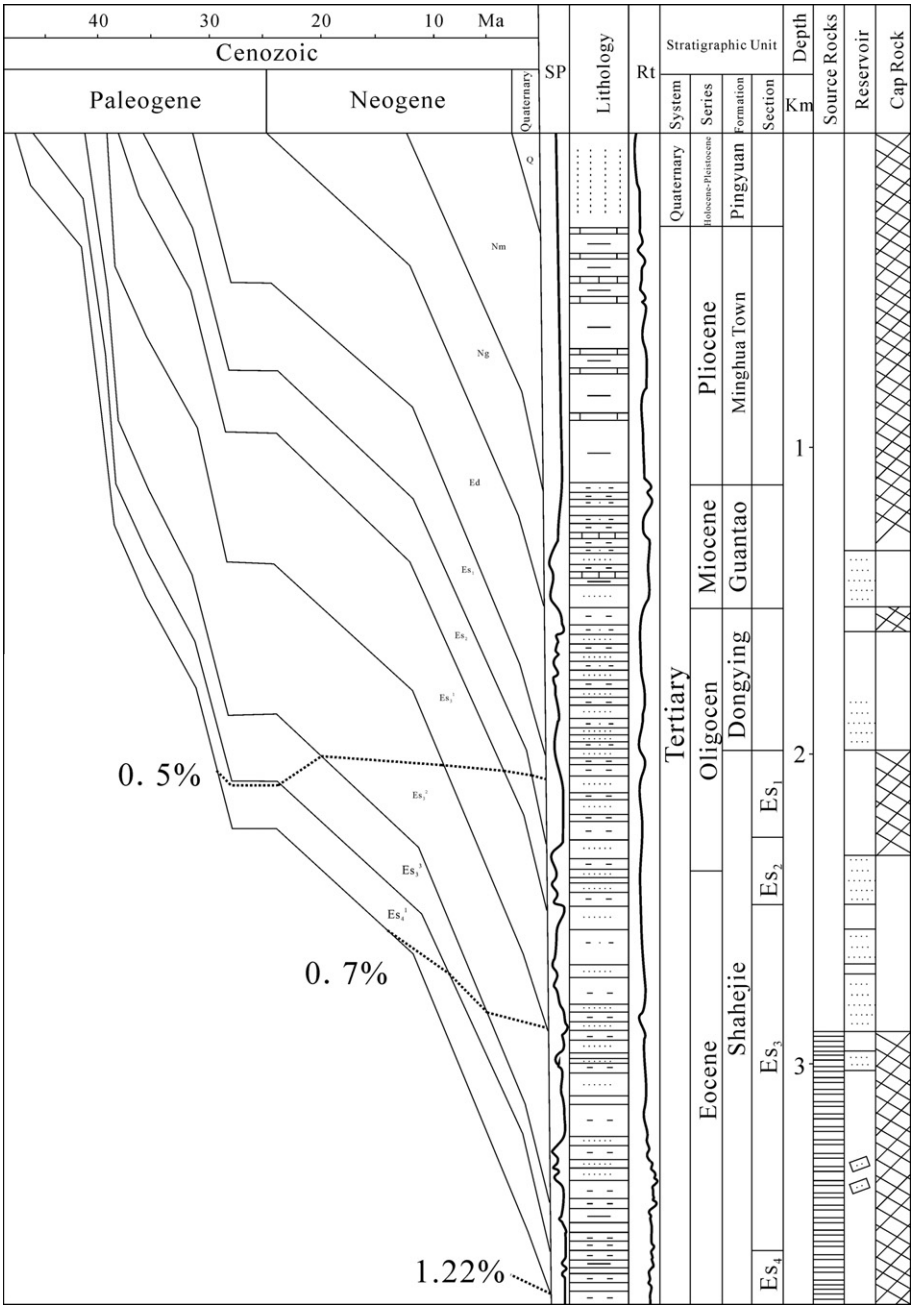

Fig. 4. Burial history of source rocks in Niu11 well, Niuzhuang Sag, Dongying Depression, Bohai Bay Basin, China (modified after Zhang and Zhang, 1999).

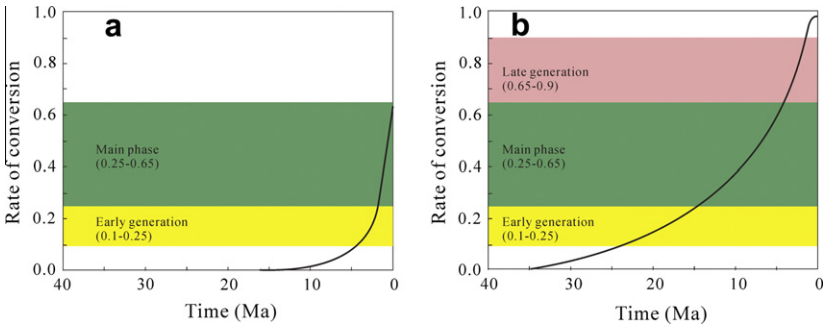

Fig. 5. Total hydrocarbon generation history for $E_{2\text{-}3}s_3^3$ (a) and $E_{2\text{-}3}s_4^1$ source rocks (b).

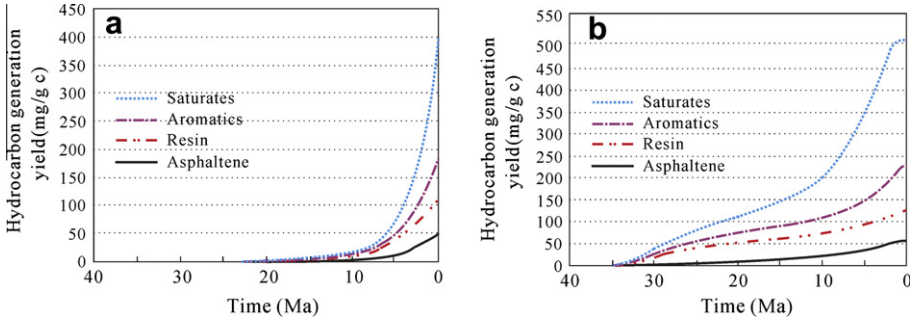

Fig. 6. Superimposed cumulative hydrocarbon yield vs. geological time curves, showing generation history of hydrocarbon fractions from $E_{2\text{-}3}s_3^3$ (a) and $E_{2\text{-}3}s_4^1$ source rocks (b) in Niuzhuang Sag, Dongying Depression, Bohai Bay Basin, China.

generation windows at about 4.26 Ma and 24.85 Ma ago, respectively (Fig. 5).

It has been observed that the pyrolysis products from kerogen or lignite degradation are dominated by heteroatomic compounds (i.e., compounds of nitrogen, sulfur, oxygen and heavy metals), called 'NSOs', of very high molecular weights (Tissot et al., 1971; Ishiwatari et al., 1977; Tissot and Welte, 1984; Teerman and Hwang, 1991; Lewan, 1993; Behar et al., 1997, 2003; Lewan and Ruble, 2002). The results could be confirmed by models proposed by Fitzgerald and van Krevelen (1959) for coal and by Tissot (1969), Ishiwatari et al. (1977) for kerogen, in which the NSOs ('mesophase' in Fitzgerald and van Krevelen, 1959) are primary products of kerogen decomposition and that hydrocarbons are, in fact, generated from secondary cracking of NSOs. This kinetic scheme was also proposed by Lewan (1997), whereby kerogen first decomposes into a tarry bitumen enriched in polar compounds. Then, this bitumen would undergo secondary cracking and generate the main part of the hydrocarbons. However, the data given in Table 2 and plotted in Fig. 6 do not support this reaction sequence. It is shown the polars (resins + asphaltenes) increase with the hydrocarbons (saturates + aromatics) to maximum yields, and it is not demonstrated that the two step reaction of kerogen to polar-rich bitumen and subsequent polar-rich bitumen to hydrocarbon-rich oil. In fact, the NSOs may be partially destroyed at the same time they are being generated. At present, the modeled yields of saturates, aromatics, resins and asphaltenes generated from $E_{2\text{-}3}s_3^3$ source rocks are 222.0 mg/g TOC, 71.3 mg/g TOC, 62.4 mg/g TOC and 50.0 mg/g TOC, respectively (Fig. 6a), while those from $E_{2\text{-}3}s_4^1$ source rocks are 280.9 mg/g TOC, 96.0 mg/g TOC, 66.8 mg/g TOC and 53.8 mg/g TOC, respectively (Fig. 6b).

Expulsion is controlled by the capability of kerogen to sorb (adsorb/absorb) petroleum, hence ultimately by the relative proportions of generative (reactive) vs. retentive (inert) kerogen. Pepper and Corvi (1995b) considered a value of 200 mg HC/g TOC to be an approximate minimum prerequisite for oil expulsion. Therefore, it can be estimated that oil began to be expelled from the $E_{2\text{-}3}s_3^3$ and $E_{2\text{-}3}s_4^1$ source rocks at about 1.86 Ma and 10.25 Ma ago, respectively (Fig. 6).

4.3.2. Modeling of expulsion

Volumetric solvent swelling is a method that has been widely used to characterize solvent–kerogen interaction and the macromolecular structure of various kerogens (Larsen and Li, 1994; Larsen and Li, 1997a,b; Ballice, 2003; Ballice and Larsen, 2003). The solubility of a compound in a polymer can be defined by a solubility parameter, δ, which is frequently referred to as the Hildebrand parameter (Hildebrand, 1936). The general rule is that the closer δ values for two compounds become, the better their mutual solubility would be. As a first approach (Larsen and Li, 1997b), kerogen appears to have a δ value ranging between 9.5 and 10 $(cal/cm^3)^{1/2}$. Hence, hydrocarbon compounds with δ values closest to this will be most retained by the kerogen. Generally, the swelling ratio of a polymer is related to the solubility of its structural units (polymer chains) in a given solvent. Thus, measuring the swelling ratio values of a polymer with different solvents provides means of assessing its solubility parameter δ. This procedure can also be applied to kerogen.

Ritter (2003a,b) divided liquid hydrocarbons into heavy saturates, heavy aromatics and NSOs (resins + asphaltenes), with the solubility parameter δ being 6.8 $(cal/cm^3)^{1/2}$, 8.0 $(cal/cm^3)^{1/2}$ and 9.0 $(cal/cm^3)^{1/2}$, respectively. In this study, seven solvents (*n*-hexane, o-xylene, 2,5-dimethylthiophene, acetone, vinyl acetate, propan-2-ol and ethanol) with the Hildebrand parameter (δ) ranging from 7.3 to 12.7 $(cal/cm^3)^{1/2}$ were used to obtain swelling ratio curves, which show relationships among δ value, swelling ratio and pyrolysis temperature. Fig. 7 shows the Gaussian fitted solvent swelling curves for residual kerogen at different temperatures, which indicate that the $E_{2\text{-}3}s_3^3$ source rock shows a higher retention yield than the $E_{2\text{-}3}s_4^1$ source rock.

Cai et al. (2007) and Zhang et al. (2008) employed Ritter's technique (Ritter et al., 2003a,b) to estimate hydrocarbon (HC) retention in kerogen, and observed that the retained HC seemed to be overestimated in many cases. In this study, the solubility parameter δ for the total hydrocarbon was calculated by weighting the contents of group-type fractions at the different pyrolysis temperatures with the solubility parameters δ for heavy saturates, heavy aromatics and NSOs (resins + asphaltenes), respectively.

$$\delta = \sum W_i \delta_i \quad (i = s, a, n) \tag{4}$$

where W_s, W_a and W_n are the fractions of saturates, aromatics and NSOs in total HC, respectively; δ_s, δ_a and δ_n represent the solubility parameters of heavy saturates, heavy aromatics and NSOs, respectively. So the solubility parameter δ for the total hydrocarbon at the different pyrolysis temperatures can be calculated (Appendix 2). Taking Niu15 kerogen as an example, when the pyrolysis temperature was 320 °C, the solubility parameter δ for the total hydrocarbon generated is 8.11 $(cal/cm^3)^{1/2}$, the Q_v of residual kerogen at 320 °C is 1.3070 by means of the insertion method in Fig. 7a. So the solubility parameter δ for the total hydrocarbon at the different pyrolysis temperatures was illustrated in Fig. 7 by means of the insertion method. Therefore, the Q_v of residual kerogen at different pyrolysis temperatures can be derived, and the retention yields of total hydrocarbon can then be calculated (Fig. 8a and b) by the following equation:

$$Y = \frac{(Q_v - 1.0) * \rho_1}{\rho_2} \tag{5}$$

where Y is the total hydrocarbon retention; Q_v is the swelling ratio of residual kerogen at different pyrolysis temperatures; ρ_1 and ρ_2 are the density values of total hydrocarbon and the residual kerogens, respectively, and the density of the total hydrocarbon is estimated to be 0.9 g/cm^3 in this study.

The retention yield of each oil fraction can be determined by multiplying the retention yield of total hydrocarbon with normalization of the solubility parameter δ for each group-type fraction, according to the following equation, in order to avoid overestimating the retention of this particular oil fraction:

$$Y_j = Y\delta_j / \sum \delta_i \quad (i, j = s, a, n) \tag{6}$$

where Y is the total hydrocarbon retention. Y_j is the retained yield of fraction j in the kerogen; δ_s, δ_a and δ_n represent the solubility parameters of heavy saturates, heavy aromatics and NSOs, respectively. Thus, the contents of the expelled group-type fractions of petroleum could also be computed.

In this study, in order to compare with kinetics of hydrocarbon generation and to build up the kinetic model of oil group-type generation and expulsion, we regard oil retention as a kinetic process. As the retention yields in kerogen are gradually decreased with increase in maturation/pyrolysis temperature (Fig. 8a and b), it is necessary to carry out a simple transformation when the kinetic parameters are fitted and applied to geological conditions. The kinetic parameters for retention of oil and its group-type fractions are fitted by using KINETICS 2000 software (Fig. 8c and d), following the procedures and steps similar to those for generating hydrocarbon as mentioned above. Based on the burial and thermal history of the Niuzhuang sag, the retention history of the oil and its fractions in Niuzhuang sag, Dongying Depression, Bohai Bay Basin could be simulated. Combining the generation history and retention history and coupling with the Easy%Ro model (Sweeney and Burnham, 1990), The kinetic model of hydrocarbon generation, retention and expulsion were modeled (Fig. 9), and calculated values were provided in Appendix 3. The results demonstrate that when Ro% increases to 0.75 and 0.65, the oil starts to be expelled from the $E_{2\text{-}3}s_3^3$ and $E_{2\text{-}3}s_4^1$ source rocks at about 3.96 Ma and 17.46 Ma ago, respectively, which means that the $E_{2\text{-}3}s_3^3$ and $E_{2\text{-}3}s_4^1$ source rocks are buried at a depth of 3180 m and 2600 m,

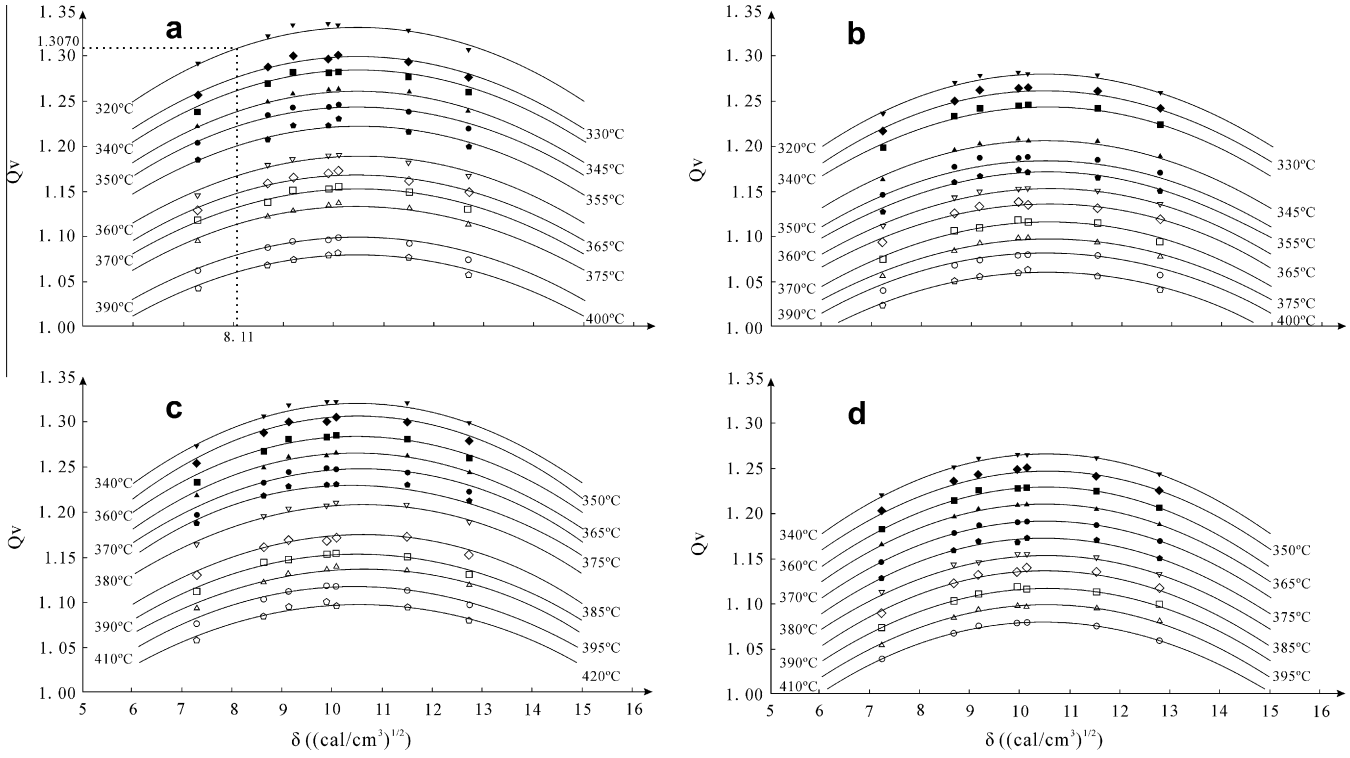

Fig. 7. Swelling ratio curves showing relationships among δ value, swelling ratio and pyrolysis temperature, with high swelling ratio suggesting high HC retaining potential (a, 2 °C/h Niu15 kerogen; b, 2 °C/h Wang120 kerogen; c, 20 °C/h Niu15 kerogen; d, 20 °C/h Wang120 kerogen).

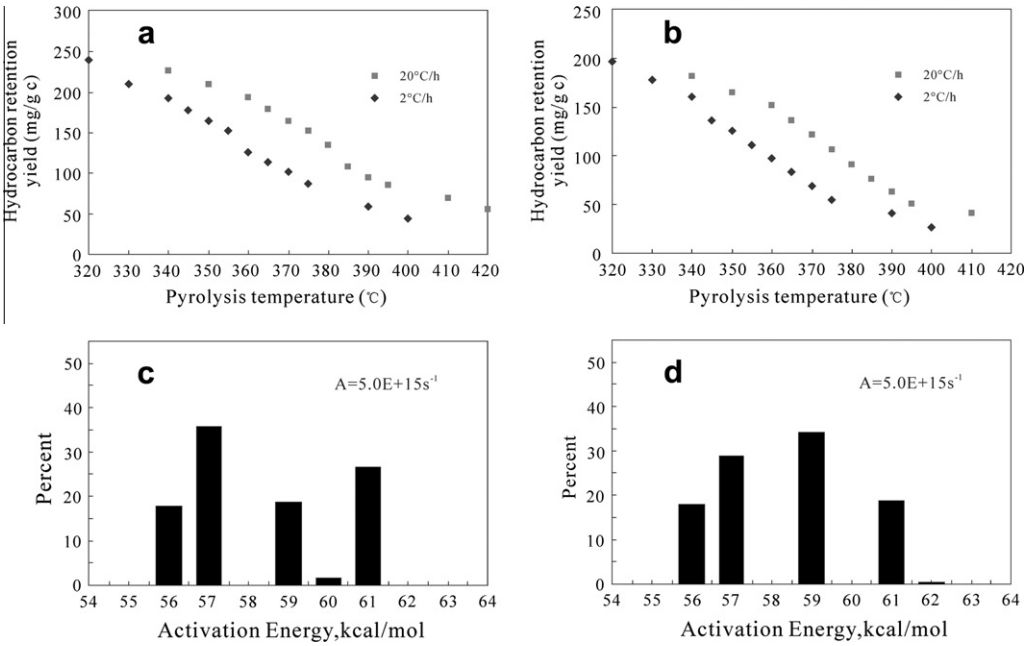

Fig. 8. Calculated retention yield of total hydrocarbon at different heating rates and kinetic parameters for total products retained in kerogens (a, Niu15; b, Wang120; c, Niu15; d, Wang120).

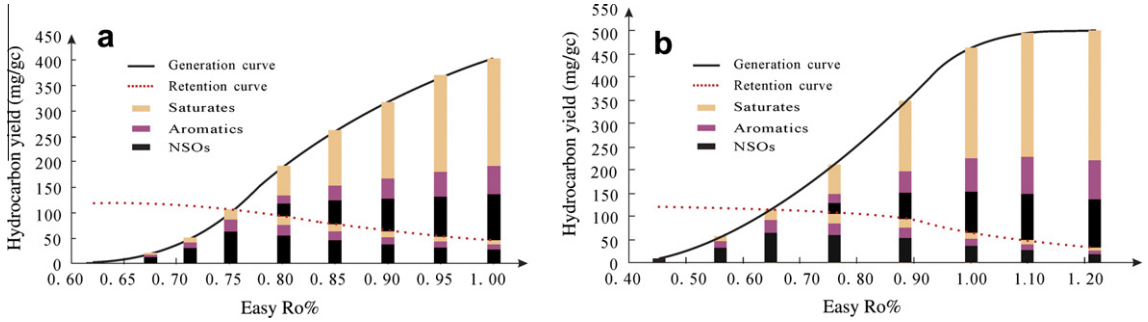

Fig. 9. Retained and expelled oil composition vs. Easy%Ro for Niuzhuang Sag, Dongying Depression, Bohai Bay Basin, China (a, $E_{2\text{-}3}s_3^3$ source rock; b, $E_{2\text{-}3}s_4^1$ source rock).

respectively. If 200 mg HC/g TOC is the minimum prerequisite for oil expulsion (Pepper and Corvi, 1995b), the generated oil would begin to be expelled from the $E_{2\text{-}3}s_3^3$ source rock and $E_{2\text{-}3}s_4^1$ source rock at about 1.86 Ma and 10.25 Ma ago, respectively (Fig. 6). As a result, it can be predicted that the present efficiency of petroleum expulsion only reaches about 50% of the target, since only saturated HC can be expelled (Fig. 9). Our results suggest that the minimum prerequisite for oil expulsion is variable and depends upon the type of source rock and the maturation and thermal history it undergoes.

As the total hydrocarbon expulsion potential increases with the increase in Ro%, the $E_{2\text{-}3}s_3^3$ and $E_{2\text{-}3}s_4^1$ source rocks reached maximum expulsion yield at 335.6 mg/g TOC and 433.3 mg/g TOC, with the corresponding Ro% values being 1.00% and 1.22%, respectively. As shown in Fig. 9, aromatics and NSO compounds demonstrate lower expulsion potential than saturates, even though the expulsion efficiency still increases gradually with increasing maturation. The proportions of the expelled saturates, aromatics and NSOs are about 60%, 15% and 25%, respectively, at present. Lu et al. (2003) studied group compositions of 20 wells crude oil samples from Dongying Depression and found that the proportions of saturates, aromatics and NSOs range between 27.0–80.0%, 9.3–6.4% and 5.7–37.8%, respectively. The study on the petroleum system of the Niuzhuang South Slope (Li et al., 2005) shows similar proportion ranges for group-type fractions. The statistical ranges of the crude oil group compositions and the predicted values are demonstrated in Fig. 10, which indicates that the predicted values are within the acceptable ranges from statistics, although the predicted NSOs value is slightly higher than that of the crude oil.

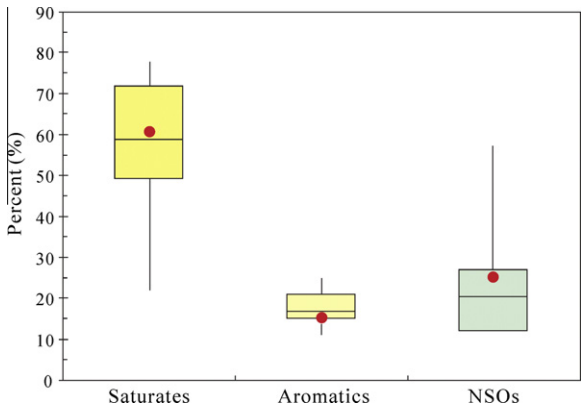

Fig. 10. The box-whisker plot for the crude oil type-group fractions (raw data from Li et al., 2005) based on the values predicted from our expulsion model (circles).

5. Conclusions

The kinetics of crude oil and its group-type fractions were studied by way of an experimental scheme and associated calculations for oil expulsion are addressed in this paper. The results of kinetic modeling show that the $E_{2\text{-}3}s_3^3$ and $E_{2\text{-}3}s_4^1$ source rocks in the Niuzhuang sag entered the "oil window" at 4.26 Ma and 24.85 Ma, respectively, the $E_{2\text{-}3}s_3^3$ source rocks are still in the main phase of hydrocarbon generation, while the $E_{2\text{-}3}s_4^1$ source rocks have nearly finished the process of oil generation. At present, the yields of saturates, aromatics, resins and asphaltenes from $E_{2\text{-}3}s_3^3$ source rocks are 222.0 mg/g TOC, 71.3 mg/g TOC, 62.4 mg/g TOC and 50.0 mg/g TOC, and those from $E_{2\text{-}3}s_4^1$ source rocks are 280.9 mg/g TOC, 96.0 mg/g TOC, 66.8 mg/g TOC and 53.8 mg/g TOC, respectively.

Our results suggest that when Ro% is 0.62 and 0.45 for $E_{2\text{-}3}s_3^3$ and $E_{2\text{-}3}s_4^1$ source rocks respectively, the NSO compounds are primarily generated and retained in the rocks; when Ro% increases to 0.75 and 0.65, the generated hydrocarbons would start to be expelled at about 3.96 Ma and 17.46 Ma ago, respectively. The expulsion potential for total hydrocarbon increases with increase in Ro%, and the $E_{2\text{-}3}s_3^3$ and $E_{2\text{-}3}s_4^1$ source rocks reach maximum expulsion yields at 335.6 mg/g TOC and 433.3 mg/g TOC, respectively, with the corresponding Ro% being 1.00% and 1.22%, respectively.

The aromatics and NSO compounds show considerably lower expulsion potentials than saturates, even though the expulsion efficiency also increases gradually with increase in maturation. The proportions of the expelled saturates, aromatics and NSOs are about 60%, 15% and 25%, respectively, at present. The method used, based on swelling experiments and kinetic modeling, could be used to predict the timing of oil expulsion and the compositions of the group-type fractions of expelled/retained oil.

Acknowledgements

The authors would like to thank Profs. J. Liu and An Xu for their help during the pyrolysis experiments. This work was supported by the NSFC (Grant No. 41173054) and the Earmarked Fund of the State Key Laboratory of Organic Geochemistry (Grant No. OGL-200914). The authors are grateful to Prof. Maxwell for the English improvements on the early manuscript. TWe would like to thank Prof. Alan Burnham and the anonymous reviewer for critical and constructive review. This is contribution No. IS-1548 from GIGCAS.

Appendix A. Supplementary material

Supplementary data associated with this article can be found, in the online version, at http://dx.doi.org/10.1016/j.orggeochem.2012.08.006.

Associate Editor—**Ken Peters**

References

Ballice, L., 2003. Solvent swelling studies of Goynuk (Kerogen Type-I) and Beypasari oil shales (Kerogen Type-II). Fuel 82, 1317–1321.

Ballice, L., Larsen, J.W., 2003. Changes in the cross-link density of Goynuk oil shale (Turkey) on pyrolysis. Fuel 82, 1305–1310.

Bastow, T.P., Van Aarssen, B.G.K., Lang, D., 2007. Rapid small-scale separation of saturate, aromatic and polar components in petroleum. Organic Geochemistry 38, 1235–1250.

Behar, F., Ungerer, P., Kressmann, S., Rudkiewicz, J.L., 1991a. Thermal evolution of crude oils in sedimentary basins: experimental simulation in a confined system and kinetic modeling. Revue de l'Institut Français du Pétrole 46, 151–181.

Behar, F., Kressmann, S., Rudkiewicz, J.L., Vandenbroucke, M., 1991b. Experimental simulation in a confined system and kinetic modeling of kerogen and oil cracking. Organic Geochemistry 19, 173–189.

Behar, F., Vandenbroucke, M., Tang, Y., Marquis, F., Espitalié, J., 1997. Thermal cracking of kerogen in open and closed systems: determination of kinetic parameters and stoichiometric coefficients for oil and gas generation. Organic Geochemistry 26, 321–339.

Behar, F., Lewan, M.D., Lorant, F., Vandenbroucke, M., 2003. Comparison of artificial maturation of lignite in hydrous and non-hydrous conditions. Organic Geochemistry 34, 575–600.

Behar, F., Roy, S., Jarvie, D., 2010. Artificial maturation of a Type I kerogen in closed system: Mass balances and kinetic modeling. Organic Geochemistry 41, 1235–1247.

Braun, R.L., Burnham, A.K., 1990. Mathematical model of oil generation, degradation, and expulsion. Energy and Fuels 4, 132–146.

Braun, R.L., Burnham, A.K., 1992. PMOD: a flexible model of oil and gas generation, cracking and expulsion. Organic Geochemistry 19, 161–172.

Braun, R.L., Burnham, A.K., Reynolds, J.G., 1992. Oil and gas evolution kinetics for oil shale and petroleum source rocks determined from pyrolysis-TQMS data at two heating rates. Energy and Fuels 6, 468–474.

Burnham, A.K., Braun, R.L., 1990. Development of a detailed model of petroleum formation, destruction and expulsion from lacustrine and marine source rocks. Organic Geochemistry 16, 27–39.

Burnham, A.K., Braun, R.L., 1999. Global kinetic analysis of complex materials. Fuel and Energy Abstracts 13, 1–22.

Cai, Y.L., Zhang, X., Zou, Y.-R., 2007. Solvent swelling: a new technique for oil primary migration. Geochimica 36, 351–356 (in Chinese with English abstract).

Chen, Z.L., Zhou, G.J., Alexander, R., 1994. A biomarker study of immature crude oils from the Shengli Oil field, People's Republic of China. Chemical Geology 113, 117–132.

Cody, G.D., Painter, E.C., 1997. Modulus of swollen coal gels. Energy and Fuels 11, 1044–1047.

Delvaux, D., Martin, H., Leplat, P., Paulet, J., 1990. Geochemical characterization of sedimentary organic matter by means of pyrolysis kinetic parameters. Organic Geochemistry 16, 175–187.

Dieckmann, V., 1998. Zur Vorhersage der Erdöl- und Erdgaszusammensetzungen durch die Integration von Labor- und Fallstudien. PhD Thesis Forschungszentrum Jülich, 285 pp.

Dieckmann, V., 2005. Modelling petroleum formation from heterogeneous source rocks: the influence of frequency factors on activation energy distribution and geological prediction. Marine and Petroleum Geology 22, 375–390.

Dieckmann, V., Caccialanza, P.G., Galimberti, R., 2002. Evaluating the timing of oil expulsion: about the inverse behaviour of light hydrocarbons and oil asphaltene kinetics. Organic Geochemistry 33, 1501–1513.

Editing Committee of Chinese Petroleum Geology, 1987. Chinese Petroleum Geology (2)-Shengli Oil Field. Petroleum Industry Press, Beijing, pp. 78–99 (in Chinese).

Fitzgerald, D., Van Krevelen, D.W., 1959. Chemical structure and properties of coal: the kinetics of coal carbonization. Fuel 38, 17–37.

Hamurcu, E., Baysal, B.M., 1993. Interpenetrating polymer networks of poly (dimethylsiloxane): 1. Preparation and characterization. Polymer 34, 5163–5167.

Han, Z., Kruge, M.A., 1999. Chemistry of maceral and groundmass density fractions of torbanite and cannel coal. Organic Geochemistry 30, 1381–1401.

Hildebrand, J.H., 1936. The Solubility of Non-electrolytes. Reinhold, New York.

Horsfield, B., Schenk, H.J., Mills, N., Welte, D.H., 1992. An investigation of the in-reservoir conversion of oil to gas: compositional and kinetic findings from closed-system programmed-temperature pyrolysis. Organic Geochemistry 19, 191–204.

Houseknecht, D.W., Hayba, D.O., 1998. Modeling oil generation in the undeformed part of the arctic national wildlife refuge 1002 area. United States Geological Survey 98, 1–24.

Ishiwatari, R., Ishiwatari, M., Rohrback, B.G., Kaplan, I.R., 1977. Thermal alteration experiments on organic matter from recent marine sediments in relation to petroleum genesis. Geochimica et Cosmochimica Acta 41, 815–828.

Juntgen, H., Klein, J., 1975. Entstehung von Erdgas aus kohligen Sedimenten. Erdöl und Kohle, Erdgas, Petrochemie 28, 65–73.

Larsen, J.W., Li, S., 1994. Solvent swelling studies of Green River kerogen. Energy and Fuels 8, 932–936.

Larsen, J.W., Li, S., 1997a. Changes in the macromolecular structure of a type I kerogen during maturation. Energy and Fuels 11 (897), 901.

Larsen, J.W., Li, S., 1997b. An initial comparison of the interactions of type I and type III kerogens with organic liquids. Organic Geochemistry 26, 305–309.

Lewan, M., 1993. Laboratory simulation of petroleum formation: hydrous pyrolysis. In: Engel, M.H., Macko, S. (Eds.), Organic Geochemistry, Principles and Applications. Plenum, New York, pp. 419–442.

Lewan, M.D., 1997. Experiments on the role of water in petroleum formation. Geochimica et Cosmochimica Acta 61, 3691–3723.

Lewan, M.D., Ruble, T.E., 2002. Comparison of petroleum generation kinetics by isothermal hydrous and non-isothermal open-system pyrolysis. Organic Geochemistry 33, 1457–1475.

Li, P.L., 2004. Oil/gas distribution patterns in Dongying Depression, Bohai Bay Basin. Journal of Petroleum Science and Engineering 41, 57–66.

Li, S., Pang, X., Li, M., Jin, Z., Qiu, Q., Gao, Y., 2005. Geochemistry of petroleum systems in the Niuzhuang South Slope of Bohai Bay Basin: Part 4. Evidence for new exploration horizons in a maturely explored petroleum province. Organic Geochemistry 36, 1135–1150.

Liu, Q., Zhang, L., Shen, Z., Kong, X., Li, Z., 2003. Evolution of lake-basin types and occurrence of hydrocarbon source rocks in Dongying Depression. Acta Petrolei Sinica 25, 42–45 (in Chinese with English abstract).

Lopatin, N.V., 1971. Temperature and geologic time as factors in coalification. Akademy Nauk SSSR Izvestias Serie Geologia 3, 95–106 (in Russian).

Lu, H.Y., Xiao, X.M., Liu, Z.Y., Gao, X.L., Guo, R.T., Wang, J.B., 2003. Organic geochemistry and origin types of crude oils from the northern area of the Dongying Depression. Acta Sedimentologica Sinica 21 (4), 707–712 (in Chinese with English abstract).

Otake, Y., Suuberg, E.M., 1997. Temperature dependence of solvent swelling and diffusion processes in coals. Energy and Fuels 11, 1155–1164.

Pan, Y., Zhang, Sh., Xiao, H., 2003. Subtle Petroleum Pools Exploration in Jiyang Rift Basin. Petroleum Industry Publishing House, Beijing (in Chinese).

Pang, X.Q., Li, M.W., Li, S.M., Jin, Z.J., 2003. Geochemistry of petroleum systems in the Niuzhuang south slope of Bohai Bay Basin. Part 2: Evidence for significant contribution of mature source rocks to 'immature oils' in the Bamianhe field. Organic Geochemistry 34, 931–950.

Pepper, A.S., Corvi, P.J., 1995a. Simple kinetic models of petroleum formation. Part 1: Oil and gas generation from kerogen. Marine and Petroleum Geology 12, 291–319.

Pepper, A.S., Corvi, P.J., 1995b. Simple kinetic models of petroleum formation. Part III: Modelling an open system. Marine and Petroleum Geology 12, 417–452.

Pepper, A.S., Dodd, T.A., 1995. Simple kinetic models of petroleum formation. Part II: Oil–gas cracking. Marine and Petroleum Geology 12, 321–340.

Quigley, T.M., Mackenzie, A.S., Gray, J.R., 1987. Kinetic theory of petroleum generation. In: Doligez, B. (Ed.), Migration of Hydrocarbons in Sedimentary Basins. Editions Technip, Paris, pp. 649–665.

Reynolds, J.G., Burnham, A.K., Mitchell, T.O., 1995. Kinetic analysis of California petroleum source rocks by programmed temperature micropyrolysis. Organic Geochemistry 23, 109–120.

Ritter, U., 2003a. Fractionation of petroleum during expulsion from kerogen. Organic Geochemistry 78–79, 417–420.

Ritter, U., 2003b. Solubility of petroleum compounds in kerogen: implications for petroleum expulsion. Organic Geochemistry 34, 319–326.

Sandvik, E.I., Young, W.A., Curry, D.J., 1992. Expulsion from hydrocarbon sources: the role of organic absorption. Organic Geochemistry 19, 77–87.

Schenk, H.J., Horsfield, B., 1998. Using natural maturation series to evaluate the utility of parallel reaction kinetics models: an investigation of Toarcian shales and Carboniferous coals, Germany. Organic Geochemistry 29, 137–154.

Schenk, H.J., di Primio, R., Horsfield, B., 1997a. The conversion of oil into gas in petroleum reservoirs. Part I: Comparative kinetic investigation of gas generation from crude oil of lacustrine, marine and fluviodeltaic origin by programmed temperature closed-system pyrolysis. Organic Geochemistry 26, 467–481.

Schenk, H.J., Horsfield, B., Krooss, B., Schaefer, R.G., Schwochau, K., 1997b. Kinetics of Petroleum Formation and Cracking, Petroleum and Basin Evolution: Insights from Petroleum Geochemistry, Geology and Basin Modeling. Springer, Berlin, Federal Republic of Germany.

Sundararaman, P., Merz, P.H., Mann, R.G., 1992. Determination of kerogen energy distribution. Energy and Fuels 6, 793–803.

Sweeney, J.J., Burnham, A.K., 1990. Evaluating of a simple model of vitrinite reflectance based on chemical kinetics. American Association Petroleum Geologists Bulletin 74, 1559–1570.

Takanohashi, T., Yanagida, T., Iino, M., 1996. Extraction and swelling of low rank coals with various solvents at room temperature. Energy and Fuels 10, 1128–1132.

Takanohashi, T., Nakamura, K., Terao, Y., Iino, M., 2000. Computer simulation of solvent swelling of coal molecules: effects of different solvents. Energy and Fuels 24, 393–399.

Tang, Y., Jenden, P.D., Nigrini, A., Teerman, S.C., 1996. Modeling early methane generation in coal. Energy and Fuels 10, 659–671.

Teerman, S.C., Hwang, R.J., 1991. Evaluation of the liquid hydrocarbon potential of coal by artificial maturation techniques. Organic Geochemistry 17, 749–764.

Tissot, B., 1969. Premières données sur les mécanismes et la cinétique de la formation du pétrole dans les bassins sédimentaires. Simulation d'un schéma réactionnel sur ordinateur. Oil and Gas Science and Technology 24, 470–501.

Tissot, B.P., Espitalié, J., 1975. L' évolution de la matière organique des sédiments: application d'une simulation mathématique. Revue de l'Institut Français du Pétrole 30, 743–777.

Tissot, B.P., Welte, D.H., 1984. Petroleum Formation and Occurrence. Springer, Berlin.

Tissot, B., Califet-Debyser, Y., Deroo, G., Oudin, J.L., 1971. Origin and evolution of hydrocarbons in Early Toarcian shales. American Association of Petroleum Geologists Bulletin 55, 2177–2193.

Tissot, B.P., Deroo, G., Hood, A., 1978. Geochemical study of the Uinta Basin: formation of petroleum from the Green River Formation. Geochimica et Cosmochimica Acta 42, 1469–1486.

Tissot, B.P., Pelet, R., Ungerer, P., 1987. Thermal history of sedimentary basins, maturation indices, and kinetics of oil and gas generation. American Association of Petroleum Geologists Bulletin 71, 1445–1466.

Ungerer, P., 1990. State of the art of research in kinetic modeling of oil formation and expulsion. Organic Geochemistry 16, 1–25.

Ungerer, P., Pelet, R., 1987. Extrapolation of the kinetics of oil and gas formation from laboratory experiments to sedimentary basins. Nature 327, 52–54.

Vandenbroucke, M., Behar, F., Rudkiewicz, J.L., 1999. Kinetic modelling of petroleum formation and cracking; implications from the high pressure/high temperature Elgin Field (UK, North Sea). Organic Geochemistry 30, 1105–1125.

Wang, B., Qian, K., 1992. Geological Research and Exploration Experiences in Shengli Oil Field. Publishing House of Chinese Petroleum University, Dongying (in Chinese with English abstract).

Waples, D.W., 2000. The kinetics of in-reservoir oil destruction and gas formation: constraints from experimental and empirical data, and from thermodynamics. Organic Geochemistry 31, 553–575.

Welte, D.H., Yalcin, M.N., 1988. Basin modeling a new comprehensive method in petroleum geology. Organic Geochemistry 13, 141–151.

Xu, S.P., Sun, Y.G., 2006. Micro-column chromatography for the separation of compound-grouped fractions of sedimentary organic matter. Geochimica 35, 681–688 (in Chinese with English abstract).

Zhang, L.Y., Zhang, C.R., 1999. Formation Mechanism of Low-maturity Petroleum and Petroleum System. Beijing. Geological Publishing House, pp. 100–130 (in Chinese).

Zhang, L., Kong, X., Zhang, Ch., Zhou, W., Xu, X., Li, Z., 2003. High-quality oil-prone source rocks in Jiyang Depression. Geochimica 32, 35–42 (in Chinese with English abstract).

Zhang, S., Wang, Y., Shi, D., Xu, H., Pang, X., Li, M., 2004. Fault-fracture mesh petroleum plays in the Jiyang Superdepression of the Bohai Bay Basin, Eastern China. Marine and Petroleum Geology 21, 651–668.

Zhang, X., Zou, Y.-R., Cai, Y.L., Zhao, C.Y., Liu, J.Z., 2008. Retention potential of oil group-type in coals. Geochimica 37, 233–238 (in Chinese with English abstract).

Zhang, L.Y., Liu, Q., Zhu, R.F., Li, Z., Lu, X.C., 2009. Source rocks in Mesozoic–Cenozoic continental rift basins, East China: a case from Dongying Depression, Bohai Bay Basin. Organic Geochemistry 40, 229–242.